Transportation Infrastructure Geotechnology (2021) 8:114–141
https://doi.org/10.1007/s40515-020-00118-7

TECHNICAL PAPER

Probabilistic Analysis of Slopes with Linearly Increasing Undrained Shear Strength Using RLEM Approach

Sina Javankhoshdel[1] · Brigid Cami[2] · Reza Jamshidi Chenari[3] · Pooya Dastpak[4]

Accepted: 17 July 2020 / Published online: 25 July 2020

Abstract

Shear strength parameters in naturally alluvial deposits bear variation with depth (non-stationarity). Probabilistic analysis of simple slopes with linearly increasing (mean) undrained shear strength with depth and spatial variability is explored using the 2D random limit equilibrium method (RLEM) along with the non-circular failure surface assumption. A deterministic factor of safety design chart method is extended to express margins of safety as probability of failure for soils with random variability and positive correlation between shear strength parameters and unit weight. The effects of isotropic and anisotropic spatial variability and cross-correlation of soil properties on probability of failure are also investigated. Combinations of low correlation length and positive cross-correlation between strength parameters are shown to reduce the probability of failure. This offers the possibility to bring probabilistic estimates of failure into alignment with expectations of slope stability based on experience with factors of safety. The results of a limited number of RLEM analyses are compared with some other results using the 2D random finite element method (RFEM). The influence of different involved parameters and assumptions, more specifically the nonlinear variation of the undrained cohesion and also the non-circular slip surface, on the embedded uncertainty and probability of failure was elaborated. The research has emphasized the importance of non-circular failure surface assumption along with the consideration of non-stationarity in shear strength parameters.

Keywords Linearly increasing shear strength · Spatial variability · RLEM · Non-circular LEM

Electronic supplementary material The online version of this article (https://doi.org/10.1007/s40515-020-00118-7) contains supplementary material, which is available to authorized users.

✉ Reza Jamshidi Chenari
jamshidi_reza@guilan.ac.ir

Extended author information available on the last page of the article

1 Introduction

Stability analyses of slopes with linearly increasing undrained shear strength with depth and simple geometry have been reported by Gibson and Morgenstern (1962) and Hunter and Schuster (1968). These early treatments used classical circular slip analysis based on limit equilibrium methods (LEM). The same general problem was explored further by Koppula (1984) and Shen and Brand (1985). Yu et al. (1998) compared the results of finite element lower bound limit analysis and limit equilibrium method analysis for the case of slopes with linearly increasing undrained shear strength with depth. Griffiths and Yu (2015) revisited the same problem and showed that stability number N, first introduced by Taylor (1937), is greatly affected by the depth ratio D representing the ratio of height of slope above a firm stratum to height of slope H. Griffiths and Yu (2015) generated stability charts based on moment limit equilibrium for the case of linearly increasing undrained shear strength and different values of depth ratio D.

Soil properties for natural slopes have random and spatial variability as a result of the geological processes that produced them (Phoon and Kulhawy 1999). The influence of random variability of soil strength parameters on probability of failure of slopes using conventional limit equilibrium slip circle analysis has been explored by Li and Lumb (1987), Chowdhury and Xu (1993), Christian et al. (1994), Low et al. (1998), Hassan and Wolff (1999), Griffiths and Fenton (2004), Hong and Roh (2008), Ching et al. (2009), Mbarka et al. (2010) and Javankhoshdel and Bathurst (2014, 2016).

The influence of spatial variability of soil properties on probability of failure using conventional limit equilibrium slope stability analyses and random field generation techniques has been investigated by Li and Lumb (1987), Mostyn and Soo (1992), Christian et al. (1994), El-Ramly et al. (2002), Low (2003), Sirvakumar Babu and Mukesh (2004), Low et al. (2007), Hong and Roh (2008), Cho (2010), Wang et al. (2011), Tabarroki et al. (2013), Javankhoshdel and Bathurst (2014), Javankhoshdel (2016), Jamshidi Chenari and Zamanzadeh (2016), Javankhoshdel et al. (2016) and Shah Malekpoor et al. (2020). Griffiths and Fenton (2004) and Griffiths et al. (2009) presented the results of probabilistic analysis of simple slopes using 2D RFEM, which combines the finite element method, strength reduction technique and Latin hypercube sampling (LHS) of soil properties from random fields that are generated using the local average subdivision (LAS) method. Jamshidi Chenari and Zamanzadeh (2016) elaborated on the effect of both deterministic (linear) and stochastic variations of undrained shear strength on probability of failure of unsupported vertical cuts. They made comparisons between RLEM and 2D random finite difference method (RFDM) results.

Possible correlations between random shear strength parameters that can influence the computed probability of failure of a slope have been noted by Nguyen and Chowdhury (1985). These correlations are quantified by the cross-correlation coefficient (ρ). A positive correlation between s_u and γ is a reasonable expectation for cohesive soils, and positive values have been reported in the literature (e.g. Sivakumar Babu and Srivastava 2007).

Javankhoshdel and Bathurst (2016) investigated the influence of cross-correlation between random variable soil strength parameters in cohesive soil slopes using a closed-form limit equilibrium–based solution following the well-known Taylor (1937) equation. They showed that increasing the value of positive cross-correlation

coefficient between s_u and γ reduces the value of probability of failure. Earlier, Ranjbar Pouya et al. (2014) investigated the influence of cross-correlation between internal friction angle and cohesion random fields on bearing capacity of shallow footings rested on spatially variable soil deposits.

Javankhoshdel et al. (2016) extended their earlier works (Javankhoshdel and Bathurs 2014 and Javankhoshdel and Bathurst 2016) to investigate the influence of isotropic and anisotropic spatial variability of soil strength parameters on probability of failure for simple slopes with stationary mean undrained shear strength. However, the main focus of their study was on the influence of method of analysis on numerical outcomes. They compared results using (one dimensional) 1D circular LEM, 2D circular LEM, and 2D RFEM. Jamshidi Chenari and Zamanzadeh (2016) made similar comparisons between 1D circular and non-circular LEM and 2D RFDM. For the anisotropic case, Javankhoshdel et al. (2016) varied horizontal spatial correlation lengths while keeping vertical spatial correlation lengths constant, and then the reverse. They concluded that probability of failure is more sensitive to changes in vertical spatial correlation length than changes in horizontal spatial correlation length.

Jamshidi Chenari and Alaie (2015) reported some important findings on the effects of anisotropy in correlation structure on the stability of undrained clay slopes. They demonstrated a mixed effect of the heterogeneity anisotropy on reliability index depending on the deterministic factor of safety adopted. More recently, Jamshidi Chenari and Mahigir (2014) delineated a clear distinction between mechanical and heterogeneity anisotropies. They associated directionality of shear strength parameters with the mechanical anisotropy and incorporated different horizontal and vertical correlation lengths into a term defined as the heterogeneity anisotropy.

Tabarroki et al. (2013) investigated LEM circular and non-circular slope stability analyses in combination with spatially variable shear strength (RLEM) and uncorrelated soil properties. They also compared numerical outcomes with results using 2D RFEM. They concluded that circular slip analyses such as the simplified Bishop method cannot be assumed to find the most critical failure mechanisms in slopes with spatially random strength. They suggested that LEM slope stability analysis results with random fields may only be reliable using non-circular LEM with a suitably selected minimum number of vertices describing the geometry of each non-circular failure trial. Javankhoshdel et al. (2016) also showed that large differences in estimates of probability of failure using 2D RLEM and 2D RFEM approaches with spatially random soil properties were possible for slopes with simple geometry. The explanation for the differences reported in the related literature is the additional freedom available in the 2D RFEM approach to seek out more critical failure mechanisms (compared with constrained circular slip mechanisms) leading to larger computed probabilities of failure.

Griffiths et al. (2015) and Zhu et al. (2017) extended the results of prior RFEM analyses of simple slopes with constant mean (stationary) undrained shear strength to the case of linearly increasing (non-stationary) strength. The influence of possible correlations between soil properties on probabilities of failure was not considered in their study. Li et al. (2014) investigated the influence of linearly increasing (non-stationary) undrained shear strength on stability of infinite slopes. They concluded that

probability of failure will be over-estimated if statistical characteristics describing linearly increasing soil shear strength with depth are ignored.

Notwithstanding the observations made above, the use of LEM circular slip analyses for simple cohesive slopes remains familiar to practitioners. Also, with the new available optimization techniques in non-circular slope stability analysis to locate the surface corresponding to minimum factor of safety, it is possible to find the same factor of safety and the weakest failure path as FEM using non-circular LEM. Design charts based on conventional limit equilibrium methods that extend the case of constant undrained shear strength soil slopes (e.g. Taylor 1937) to cases with linearly increasing strength with depth (Hunter and Schuster 1968**;** Griffiths and Yu 2015) are useful extensions to these earlier charts. However, they are currently available only in a conventional factor of safety format. Recasting analysis results by Griffiths and Yu (2015) for linearly increasing undrained shear strength with depth into a probabilistic LEM framework was one motivation for the current study.

In this study, probabilistic analysis of simple and layered slopes with linearly increasing (non-stationary) mean undrained shear strength with depth are investigated. Included in analyses is the influence of spatial variability of soil properties with and without cross-correlation between soil input parameters. Analyses are carried out using the 2D circular and non-circular RLEM approaches. Some comparisons between the results of the 2D non-circular RLEM, the 2D circular RLEM and the 2D RFEM analyses are also presented.

2 Slope Models

There are three main schemes of undrained strength variation, which can be defined as a function of depth in Slide2 2018: depth from the top of the layer, where the depth is measured from the top of the material layer that is local to the slice, to the centre of a slice base **(**Fig. 1a**)**; distance to slope; cohesion is a function of depth, where depth is a vertical distance measured from atop of the slope to the centre of a slice base **(**Fig. 1b**)**; and depth from horizontal datum; cohesion is a function of depth, where depth is measured from a user-specified datum (y-coordinate) to the centre of a slice base **(**Fig. 1c**)**. The first two methods can be used when the slope is formed naturally, while the third method can be performed when there is an artificial slope (slope made by excavation).

The linearly varying undrained shear strength assumption is generally inferred from the literature by investigating a repertoire of in situ test data. Bjerrum (1954) has comprehensively discussed this issue for clay deposits. Recently, Jamshidi Chenari et al. (2014) have reviewed the literature on this issue and also implemented this trend of variation to the classic bearing capacity problem of shallow footings.

In this study, in order to replicate the results obtained by Griffiths and Yu (2015)**,** the undrained strength was defined based on the depth from horizontal datum. Figure 1c shows the slope model geometry where $H = 10$ m is the slope height, $\beta = 15^{o}$ is the slope angle, D = depth ratio, $s_{u0} = 20$ kPa is the undrained shear strength at crest level ($z = 0$) and $r_{su} = 1$ kPa/m is the strength density which is the gradient at which the

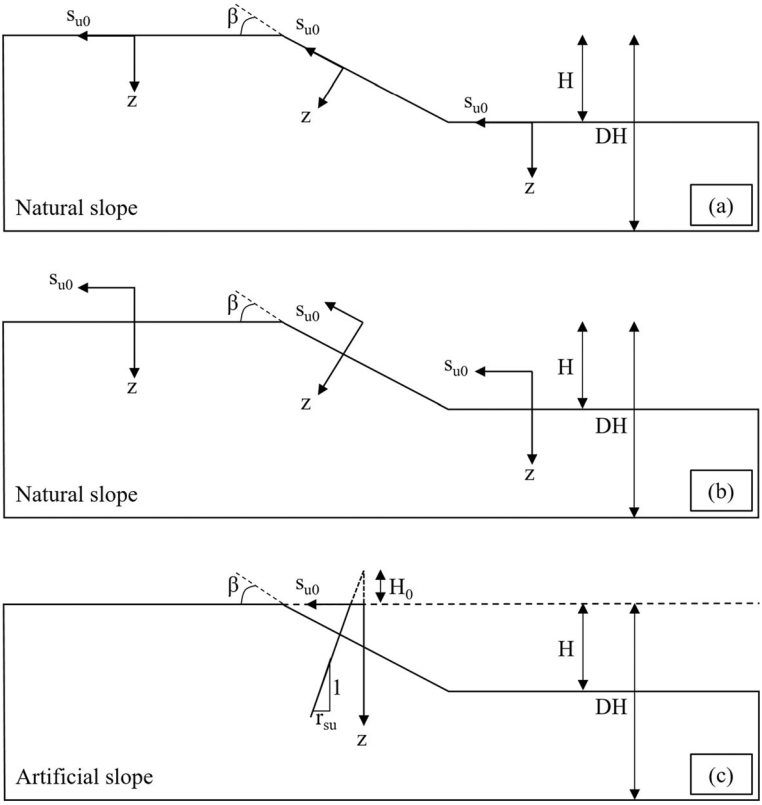

Fig. 1 Slope with linearly (mean) increasing undrained shear strength

strength trend (mean) increases with depth z. The parameter H_0 is the height above the crest at which the extrapolated undrained shear strength approaches 0 (Yu et al. 1998; Griffiths and Yu 2015).

Figure 2a and b are the slope models for the case of a two-layer slope with linearly increasing cohesive strength in both layers. The top layer in these cases is the same as the slope shown in Fig. 1 ($s_{u0} = 20$ kPa, $r_{su} = 1$ kPa/m and $\beta = 15^o$). For the two-layer cases, two different foundation heights are assumed ($D = 1.25$ and $D = 2$). In all cases, $r_{su} = 1$ kPa/m was assumed through the slope and foundation layers; therefore, assuming the value of the undrained cohesion at the top of the slope (s_{u0}) is 20 kPa, the value of cohesion at the top of the foundation layer (s_u) becomes 30 kPa. For each foundation height, two different foundation strengths are considered in this example: $s_{uW0} = 15$ kPa (weak foundation) and $s_{uS0} = 40$ kPa (strong foundation). In Fig. 2a and b, s_{uW0} and s_{uS0} are undrained shear strength at the top of the weak and strong foundations, respectively.

3 Deterministic Slope Stability Analysis with Linearly Increasing Undrained Shear Strength

In this study, the unit weight γ is assumed to be constant. In Figs. 1 and 2, undrained strength at depth z is computed as:

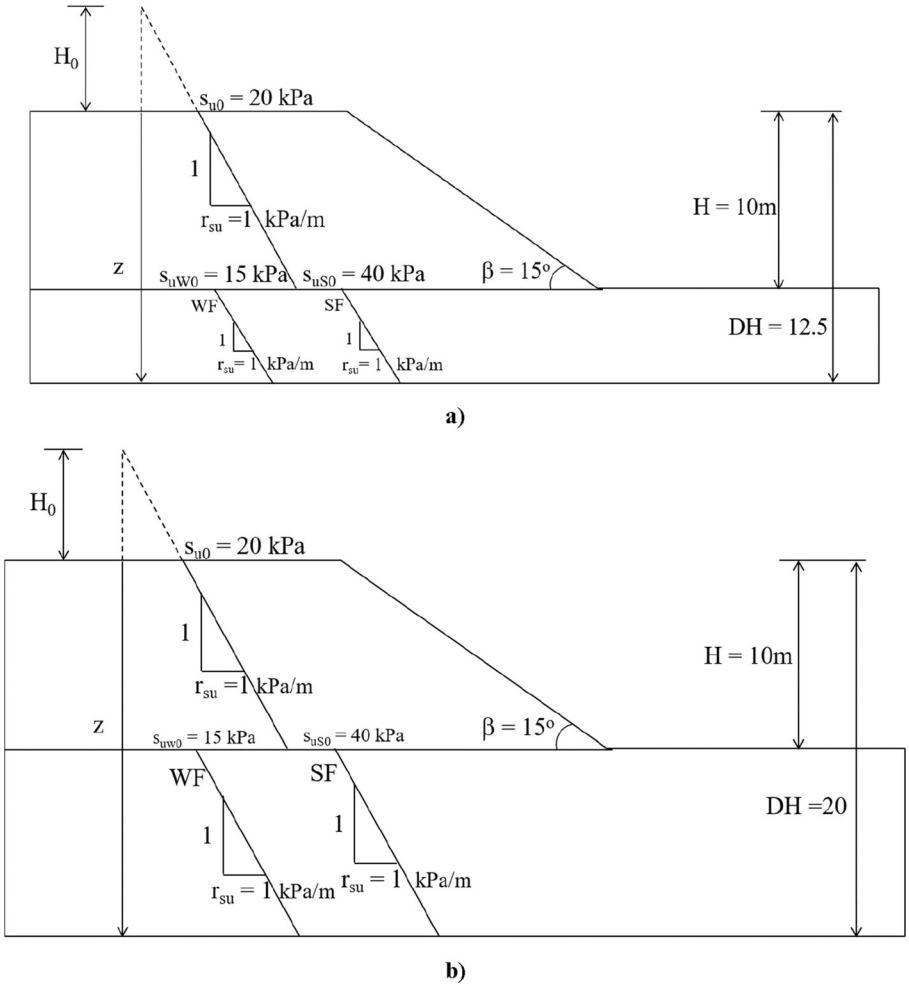

Fig. 2 Two-layer slope model: **a** D = 1.25 and **b** D = 2. (WF = weak foundation and SF = strong foundation)

$$s_u(z) = s_{u0} + r_{su}z \tag{1}$$

Hunter and Schuster (1968) introduced a dimensionless strength gradient parameter M, defined as:

$$M = \frac{H_0}{H} \tag{2}$$

which can also be written as:

$$M = \frac{s_{u0}}{r_{su}H} \tag{3}$$

Hence $M = \infty$ corresponds to the case with constant undrained shear strength assumed in the original Taylor (1937) charts. Hunter and Schuster (1968) produced charts of dimensionless stability number N as a function of β, D and M. The stability number N is proportional to the factor of safety, F_s, as follows:

$$F_s = \frac{N r_{su}}{\gamma} \tag{4}$$

Hunter and Schuster's charts show that N is strongly influenced by β and M, but only marginally affected by ratio D. Griffiths and Yu (2015) showed that values of N computed in their study for large values of D were in agreement with the results of Hunter and Schuster (1968). However, the values of N computed for smaller values of D could be considerably greater. Griffiths and Yu (2015) showed that their stability charts were in good agreement with the results of FEM analyses. In the current study, the N values from Griffiths and Yu (2015) are used based on these observations.

Slide2 2018 (Rocscience Inc. 2018) was used to carry out probabilistic and deterministic analysis of slopes with $M \geq 0$ and $r_{su} \geq 0$. Circular and non-circular LEM approaches used in this study to carry out deterministic part of the analysis which will be explained later in the paper. Figure 3 illustrates the difference between these three methods for both non-circular and circular slip surface considering various ranges of D. As seen in this figure, for an artificial slope, the stability N number is more than the natural slopes. Furthermore, Fig. 4 shows a good agreement between computed stability N numbers reported by Griffiths and Yu (2015) and results using the LEM method (circular and non-circular) in the current study. This gives confidence in the accuracy of the underlying deterministic method used in this study.

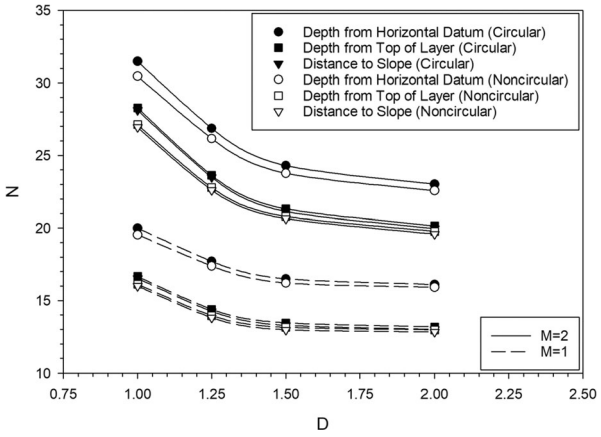

Fig. 3 Stability number N versus depth D ratio for slopes with linearly increasing undrained strength considering three different methods, and β = 15°, and M = 1 and 2

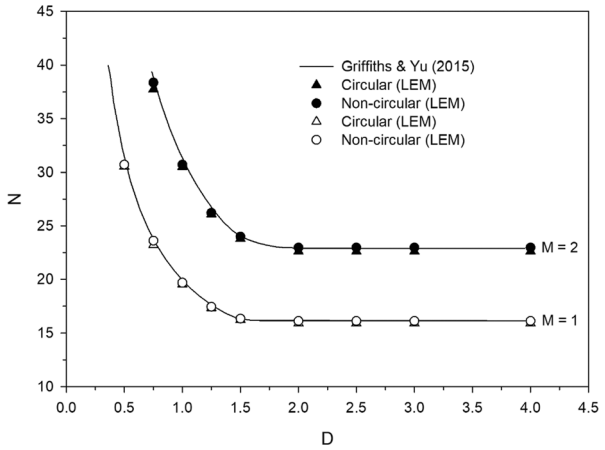

Fig. 4 Stability number N from current study and Griffiths and Yu (2015) versus depth D ratio for slopes with linearly increasing undrained strength and $\beta = 15°$, and M = 1 and 2

4 Probabilistic Analysis of Slopes with Random Soil Variability Using Combined Limit Equilibrium Method and LHS Simulation

The overall slope stability method is used which means that the factor of safety for each trial slip surface is computed with different soil property values sampled from log-normal distributions described by a mean and coefficient of variation of undrained shear strength and unit weight in each LHS. In this study, 5000 LHS were found to give an accurate estimate of the probability of failure for $P_f > 0.02\%$ for all cases.

The closed-form solution based on the first-order second moment (FOSM) approach reported by Javankhoshdel and Bathurst (2016) for the case of no spatial variability (random variability only) is also used in the current investigation to compute probabilities of failure. The closed-form solution for log-normal random variable distributions is expressed as:

$$P_f = p[F_s < 1] = \Phi\left(\frac{\ln\left(\sqrt{\frac{1+COV_{su}^2}{1+COV_\gamma^2}}/\overline{F}_s\right)}{\sqrt{\ln\left(\left(1+COV_{su}^2\right)\left(1+COV_\gamma^2\right)/\left(1+\rho COV_{su}COV_\gamma\right)^2\right)}}\right) \quad (5)$$

Here, parameters COV_{su} and COV_γ are coefficients of variation of variable s_u and γ, respectively. Parameter ρ is the cross-correlation coefficient between s_u and γ. F_s in Eq. 5 is the deterministic factor of safety estimated from Eq. 4 by assuming all parameters in average sense. Hence, the link to probabilistic estimates of the factor of safety and the deterministic factor of safety F_s is made by assigning mean values to all the soil parameters.

Equation 5 was used to generate the curves in Fig. 5 for the cases with $\rho = 0$ and 0.7 together with $COV_{su} = 0.3$ and 0.5 and $COV_{\gamma} = 0.1$. A range of F_s values was adopted by selecting different values of s_{u0}, r_{su}, and constant γ, H and D. The closed-form solution plots are illustrated for practical purposes as straight lines in semi-logarithmic scale. Superimposed on the figure are the results of LHS simulations using the circular and non-circular LEM methods with the Morgenstern-Price method with equivalent parameters' values and the case of $M = 2$ and $\beta = 15°$. There is good agreement between the two approaches which gives confidence in the use of Eq. 5 for the calculation of the probability of failure for simple slopes with linearly increasing mean undrained shear strength and constant mean unit weight.

The results in Fig. 5 show that probability of failure using Eq. 5 is independent of the magnitude of the strength density (i.e. M) and depth ratio D while maintaining a constant deterministic factor of safety F_s, acquired by adopting the parameters in an average sense. The figure also shows that:

1. The rate of change of P_f with F_s increases with decreasing the magnitude of COV_{su} while keeping the value of COV_{γ} constant.
2. When all other conditions are the same, increasing the positive correlation between s_u and γ reduces the probability of failure.
3. For the same COV_{su} and COV_{γ} values, the rate of change of P_f with F_s increases with increasing ρ.
4. For the same F_s, the parameters' correlation impact becomes more highlighted for smaller COV_{su} (and constant COV_{γ}).

The qualitative features identified at items 2 and 4 have been noted previously by Javankhoshdel and Bathurst (2016) for the case of $r_{su} = 0$.

In summary, to estimate the probability of failure using the Griffiths and Yu (2015) charts, the user first needs to compute F_s from the respective charts, and then to introduce this value into Eq. 5.

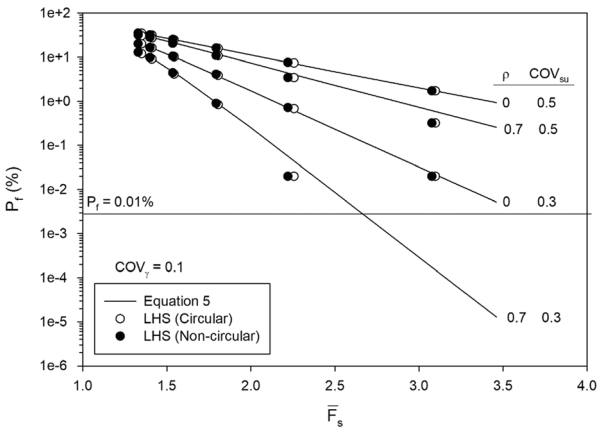

Fig. 5 Probabilities of failure (P_f) using FOSM solution (Eq. 5) and $COV_{su} = 0.5$ and 0.3, $COV_{\gamma} = 0.1$, $\rho = 0$ and 0.7

5 General Probabilistic Design Charts

As it was concluded above, Eq. 5 can be used to generate probabilities of failure for any given factor of safety for slopes with undrained shear strength linearly increasing with depth with and without cross-correlation between undrained shear strength and unit weight of the soil. Thus, it is possible to use Eq. 5 to generate general probabilistic design charts. Figures 6 and 7 show the design charts generated using Eq. 5 for COV_{su}, ranging from 0.05 to 0.5, and two cases of $COV\gamma = 0.05$ and 0.1. Figures 6 and 7 are for the cases of with and without cross-correlation between undrained cohesion and unit weight, respectively. Positive correlations of 0.1, 0.3, 0.5 and 0.7 are considered between S_u and γ and results are reported in Fig. 7a–d, respectively.

Knowing the value of the factor of safety and the COV of input parameters, and the cross-correlation between soil input properties, Figs. 6 and 7 can be used to estimate the probability of failure for design purposes. In these charts, the values of COVsu, $COV\gamma$ and ρ are within the practical range of these parameters reported in the literature. For any other values, the values of probability of failure can be interpolated from the values extracted from these charts.

It can be seen from these charts that as the COVsu becomes smaller P_f will expectedly decline. Furthermore, the influence of small $COV\gamma$ on the probability of failure is pronounced for lower values of COV_{su}, and also as the cross-correlation between S_u and γ becomes larger this influence becomes less highlighted.

Also, on these figures, for Pf = 0.01%, 0.1% and 1%, the corresponding values of reliability index are also shown. It is possible to generate design charts for the values of reliability index as well. For interested readers, these charts are also provided in a separate document as Supplementary materials.

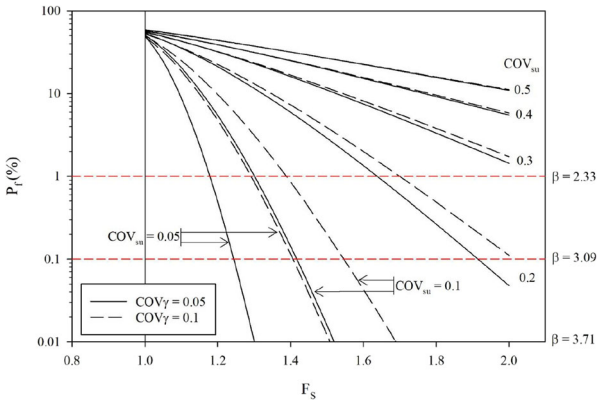

Fig. 6 Variation of probabilities of failure (P_f) versus F_S determined by Eq. 5 considering $COV_{su} = 0.05$–0.5, $COV_\gamma = 0.05$, 0.1; with no cross-correlation

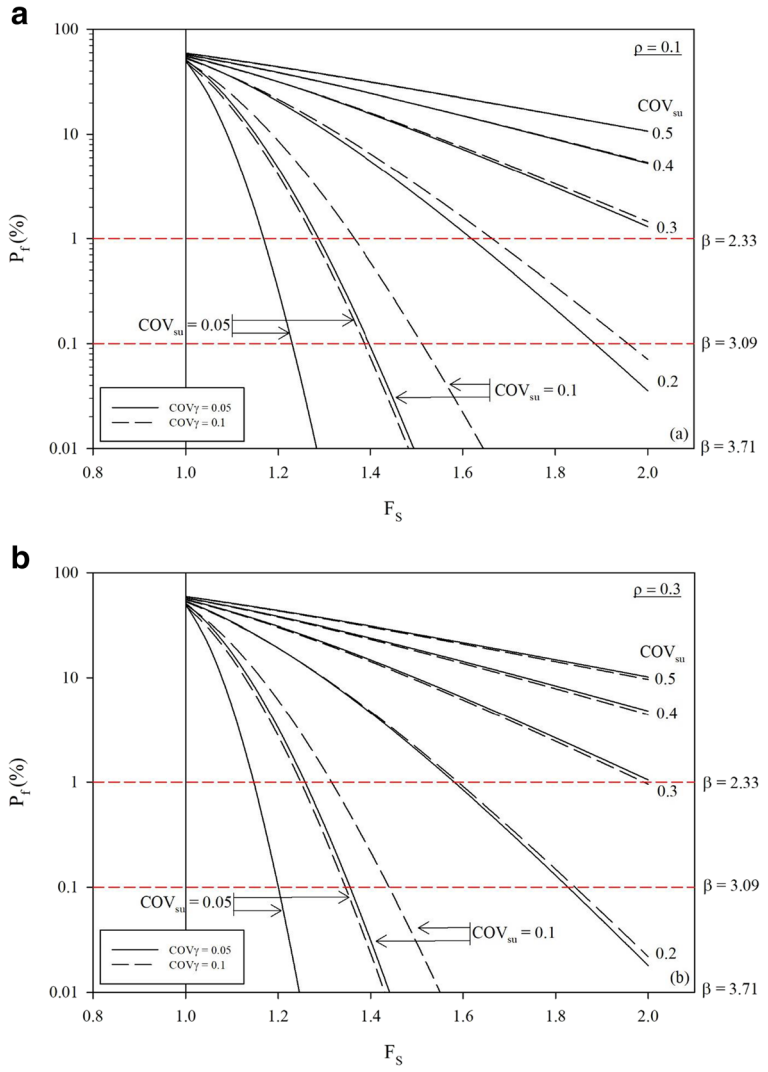

Fig. 7 Variation of probabilities of failure (P_f) versus F_S determined by Eq. 5 considering $COV_{su} = 0.05$–0.5, $COV_\gamma = 0.05$, 0.1; **a** $\rho = 0.1$, **b** $\rho = 0.3$, **c** $\rho = 0.5$ and **d** $\rho = 0.7$

6 2D RLEM Slope Stability Analyses with Spatial Variability of Soil Properties

6.1 General Approach

6.1.1 Circular RLEM

The 2D circular RLEM in this study is a combination of the deterministic LEM circular slip method using the Morgenstern-Price method combined with random soil property fields and LHS simulation as described by Javankhoshdel et al. (2016). In each LHS

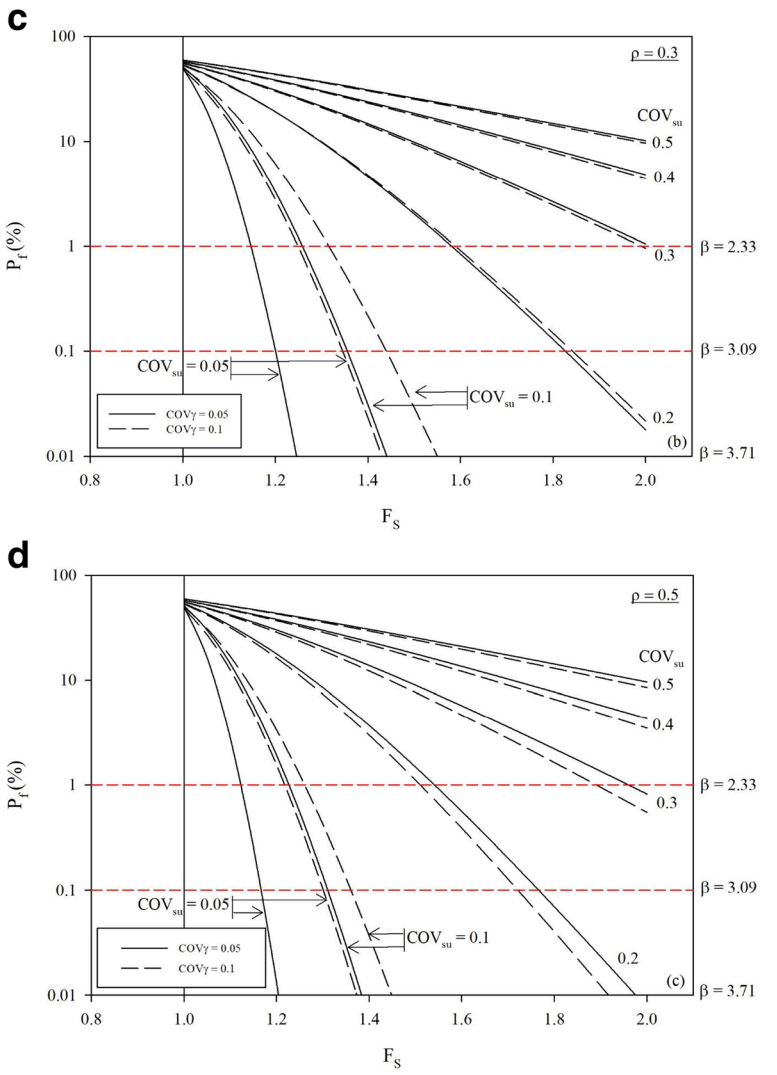

Fig. 7 (continued)

realization, a random field is generated for each soil property of interest using the local average subdivision (LAS) method (Fenton and Vanmarcke 1990) and mapped onto the slope domain comprising of a mesh of elements. The same approach has been used by Griffiths and Fenton (2004) to populate the finite element mesh used in their RFEM analyses to investigate the stability of undrained soil slopes with spatially random soil properties. Each mesh cell in the random field has a different value of soil property based on the value of the spatial correlation length for that property. LEM analysis using the Morgenstern-Price method is carried out in each LHS realization to calculate the factor of safety for the trial circular slip. The intersection of each trial circular slip with the cells in each random field determines the magnitude of s_u and γ assigned to the

base of each slice in the Morgenstern-Price method. Probability of failure is computed as the number of analyses with factor of safety $F_s < 1$ (failure) divided by the total number of LHS simulations.

The combination of a linearly increasing random field and trial circular slip mechanism using the 2D RLEM approach is shown in Fig. 8.

6.1.2 Non-circular RLEM

The non-circular RLEM used in this study is a combination of a refined search and a LEM approach (the Morgenstern-Price method). The refined search is based on circular surfaces that are converted to piece-wise linear surfaces. The search for the lowest safety factor is refined as the search progresses. An iterative approach is used so that the results of one iteration are used to narrow the search area on the slope in the next iteration.

In many cases, for the same number of surfaces, a larger number of slip surfaces with lower factors of safety were detected than the number determined from conventional grid or slope search techniques.

The refined search in this study was used together with an additional optimization technique. The optimization technique used in this paper is surface altering optimization (SAO). Surface altering optimization (SAO) technique is a novel approach to minimize the factor of safety for a given slip surface by modifying its geometry. This method, similar to the Monte Carlo random walk optimization (MCO) (Greco 1996), is a local optimization method. Although SAO can be used independently to find the critical slip surface in slope stability analysis, due to its local nature, it serves best when combined with a global search method to calculate the factor of safety. In this way, the burden of finding an approximate geometry and location of the failure surface with a minimum factor of safety is on the global search method, and then SAO modifies the geometry of that surface in a way to further minimize the factor of safety.

To attain a high flexibility for finding geometry of a critical slip surface, SAO employs spline curves in 2D. In general, spline formulation requires a larger number of parameters in comparison to the number of parameters required to describe primitive geometries such as circles. Therefore, in the grand scheme of slope stability analysis, global optimization methods can be performed using primitive surfaces to find an approximation of critical surface relatively fast followed by SAO using spline functions.

In slope stability analysis, combination of a general limit equilibrium approach such as Morgenstern-Price or Spencer slope stability method together with an optimization technique such as SAO or MCO results in a more accurate non-circular critical slip

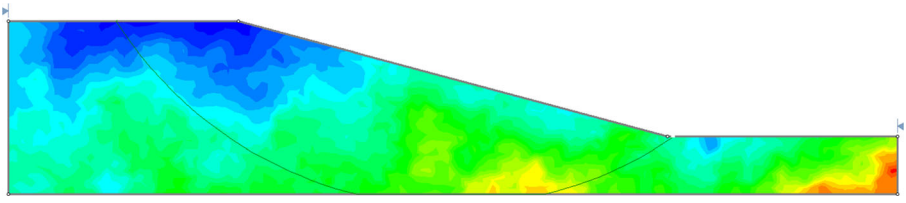

Fig. 8 Example circular slip mechanism superimposed on linearly increasing isotropic random field of soil property (e.g. s_u or γ) using RLEM

surface and its corresponding minimum factor of safety. In probabilistic analysis, this combination together with the LHS simulation results in a more accurate probability of failure.

The advantage of SAO approach over the current optimization techniques such as MCO is the accuracy of the output results and the simulation time.

The combination of refined search with optimization and random fields generated using LAS helps to locate the critical slip surface in the spatially variable field. The disadvantage of the circular RLEM is that the circular RLEM cannot capture irregular shapes of failure (Javankhoshdel et al. 2016). This is especially noticeable in cases with highly fluctuating random fields. However, the optimization technique in the non-circular RLEM moves the vertices along the slip surface to find the lowest factor of safety. Moving the vertices allows cells with lower values of soil strength in the random field mesh to be found and therefore weaker (more critical) failure paths are located.

The number of slices in the LEM part of the non-circular 2D RLEM analysis can be expected to influence numerical outcomes, particularly if the number is small (e.g. Tabarroki et al. 2013) and for smaller values of spatial correlation length. A local sub-sampling method is used in this study which is ten times sampling at the base of each slice to consider the influence of number of slices on output results. Therefore, with subsampling, 50 slices are enough.

7 RFEM

While the current study is based on numerical results using the 2D circular and non-circular RLEM, the choice of 2D RLEM or 2D RFEM on numerical outcomes is of interest particularly as prior related work by Javankhoshdel et al. (2016) has demonstrated that there can be significant differences in computed probabilities of failure between 2D circular RLEM and RFEM for otherwise nominal identical (stationary) random field conditions. In this study, the comparison between the results of non-circular RLEM and RFEM has been shown. The disadvantage of the current RFEM analysis is its inexplicably massive run time in comparison with the RLEM approach. Therefore, the comparison in this paper is only for the case of slopes with simple one-layer geometry (Fig. 1).

7.1 Effect of Spatial Variability of Soil Properties with Non-stationary Mean Undrained Shear Strength on P_f ($r_{su} > 0$)

7.1.1 General

In this section, $r_{su} > 0$ in all examples and $M = 2$ and $\beta = 15°$. The reason is that for the values of $\beta > 20°$, failure mechanisms are all toe failure type and there is no change in F_s values by changing the depth factor D. Thus, $M = 2$ and $\beta = 15°$ were selected to include the influence of D on F_s values and to be consistent with the choice of parameters in deterministic and probabilistic analyses presented earlier.

To obtain a non-stationary random field of undrained shear strength, a stationary random field is generated first based on mean and COV of undrained shear strength.

Next, the strength of each soil element was scaled to depth using the following equation:

$$c_z = c_0 \frac{\mu_{su}}{\mu_{su} + r_{su} z} \tag{6}$$

Here, c_0 is the soil strength at each element in the original stationary random field, μ_{su} is the mean strength in the original stationary random field, z is the depth of the soil element and c_z is the scaled strength in the non-stationary random field.

Figure 9 shows a random field generated for a slope with linearly increasing undrained shear strength (s_u) with depth. The random field contour can be seen to become stronger with depth.

7.2 Influence of Isotropic 2D Spatial Variability on P_f ($r_{su} > 0$)

7.2.1 Simple Slopes ($r_{su} > 0$)

For the non-circular RLEM analyses, random fields of undrained shear strength were generated for each LHS simulation and coupled with the Morgenstern-Price method as the underlying limit equilibrium method of analysis.

In most of studies which investigated the influence of spatial variability of soil properties on probability of failure, only probability of failure and deterministic factor of safety have been compared. However, another important parameter is the mean factor of safety (mean F_s). This parameter together with the probability of failure, P_f, and deterministic factor of safety, F_s, has been calculated in this study.

Figure 10 shows the results of the influence of normalized (it is not normalized) isotropic spatial correlation length (θ/H) on mean F_s and its corresponding probability of failure (P_f) for different values of depth ratio, D, by considering both auto-refine mesh and cuckoo search optimization method for non-circular slip surfaces. The plots

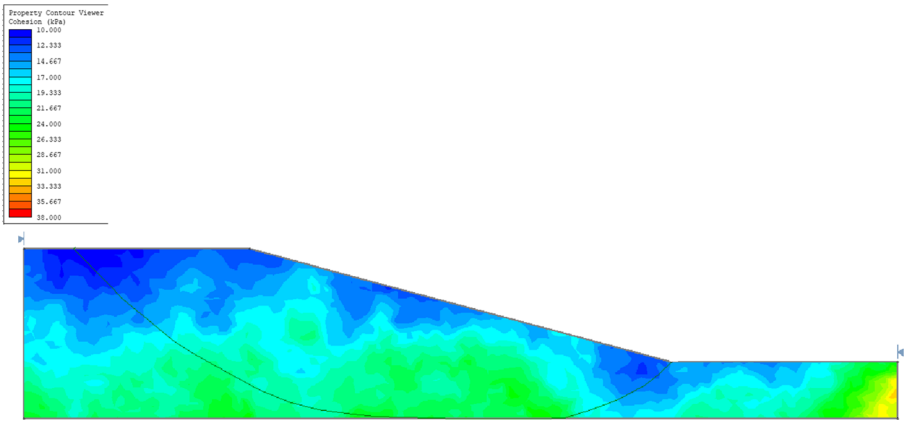

Fig. 9 Example non-circular slip mechanism superimposed on linearly increasing isotropic random field of soil property (e.g. s_u or γ) using RLEM

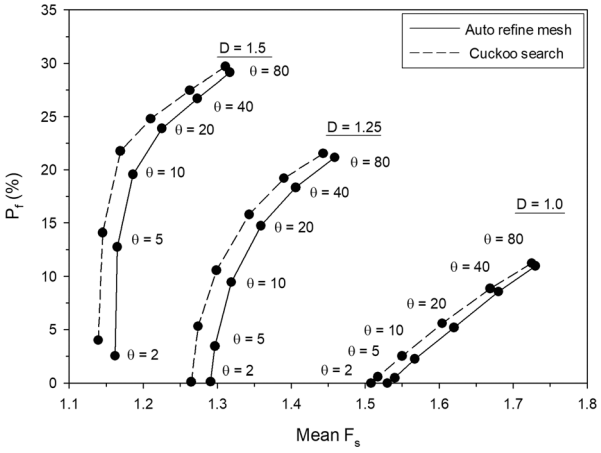

Fig. 10 P_f vs. mean F_s for different values of /H using 2D non-circular RLEM, for simple slopes with linearly increasing undrained cohesion considering both Auti refine mesh and Cuckoo search optimization

in this figure show that for the same depth ratio, the mean factor of safety increases but the probability of failure also increases as the spatial correlation length increases.

This might seem to be the opposite of general understanding of the relationship between factor of safety and probability of failure (increasing factor of safety decreases probability of failure).To explain this behaviour, Fig. 11a and b are the histograms of F_s with $\theta/H = 0.5$ and $\theta/H = 8$ at the same scale, and for $D = 1$. This figure illustrates the effect of increasing spatial variability in the analysis. The distribution of safety factor for the analyses with smaller spatial correlation length is much narrower (standard deviation of 0.33 compared with 0.69 for the larger correlation length). Even though the mean safety factor is lower (1.55 compared with 1.73), the probability of failure is also lower, due to the narrower distribution of the safety factor for the analysis with smaller spatial correlation length. In other words, as it is mentioned by Cho (2010), reducing the spatial correlation length decreases the level of uncertainty (smaller standard deviation of the F_s distribution). Although the mean F_s is also decreasing, the change in standard deviation is dominant and the COV_{Fs} (standard deviation/mean) becomes smaller (0.41 compared with 0.29) and P_f therefore decreases.

Another observation in Fig. 10 is that as the value of D decreases, for the same value of spatial correlation length, the mean value of F_s increases and the corresponding probability of failure decreases. This effect shows the influence of foundation thickness on probability of failure and mean factor of safety. In slopes with very thick foundations and undrained cohesive soil, the failure mechanism is deep. However, reducing the foundation height changes the failure geometry to a composite mechanism that has a larger factor of safety.

As previously mentioned, Tabarroki et al. (2013) argued that the circular RLEM cannot be assumed to find the most critical failure mechanisms in slopes with spatially random strength. Figure 12 shows the probabilities of failure using circular and non-circular RLEM approaches with the same spatial correlation length. All solutions were carried out with a sufficient number of LHS realizations (5000) to achieve a consistent probability of failure for each case as noted earlier. It can be seen in this figure that, as the spatial correlation length increases, the probabilities of failure calculated using both

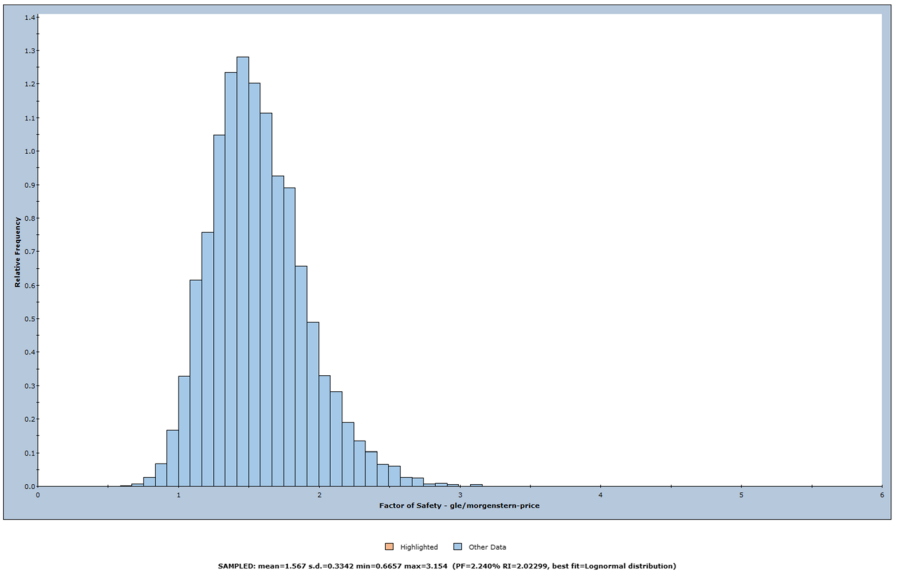

a)

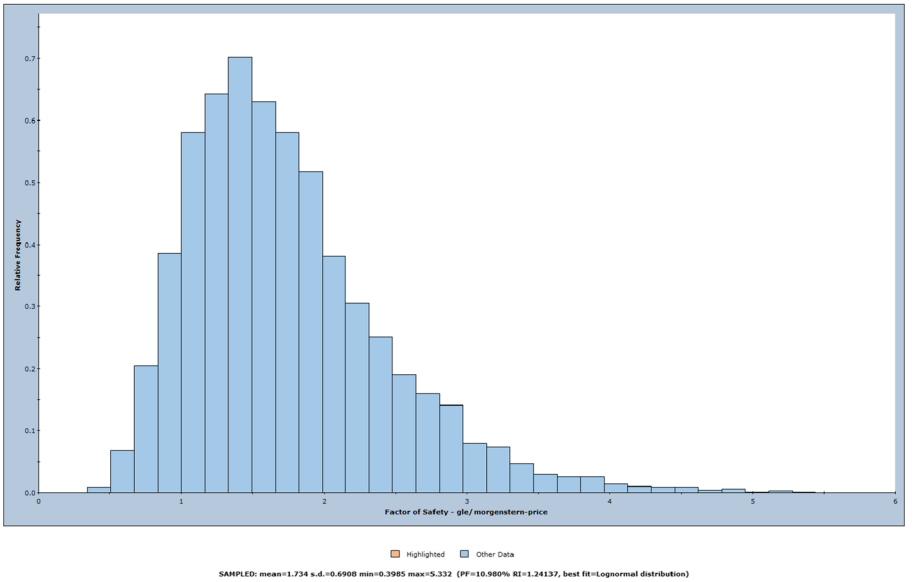

b)

Fig. 11 Histogram of F_s distribution for **a** $\theta/H = 0.5$ and **b** $\theta/H = 8$ and for $D = 1$

methods become closer. However, there are noticeable differences between the values of probability of failure using circular and non-circular RLEM approaches for smaller values of spatial correlation length (P_f is larger using the non-circular method compared with the circular method) due to the ability of the non-circular method to find weaker failure paths. This observation is in alignment with the comment by Tabarroki et al. (2013). Finally, it can be seen that for both methods, as $\theta/H \rightarrow 0$, $P_f \rightarrow 0$.

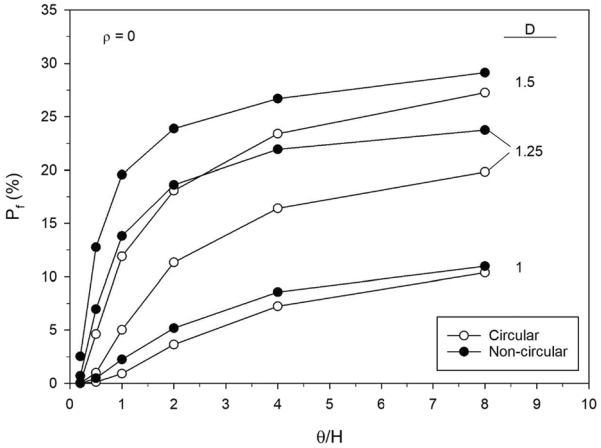

Fig. 12 Results of 2D circular and non-circular RLEM analyses of simple slopes with different D values and linearly increasing undrained cohesion

Tabarroki et al. (2013) claimed that it is possible to get the same results as the RFEM approach using non-circular RLEM analysis for the case of simple slopes. The results of analyses for simple slopes with linearly increasing undrained cohesion using non-circular RLEM and RFEM approaches is shown in Fig. 13. Again, to ensure fair comparisons, all solutions were reached through carrying out 5000 LHS realizations to warrant consistent estimations of probability of failure. It can be seen that for the same value of spatial correlation length, for some cases, the non-circular RLEM approach renders higher estimations of the probability of failure compared with the RFEM approach and for other cases, 2D RFEM results are larger. This observation can be interpreted to signify that both 2D non-circular RLEM and RFEM can find the weakest failure path in different cases. Overall, depending on the scale of fluctuation adopted, both methods are viable to outperform their counterpart by yielding higher estimations of the probability of failure.

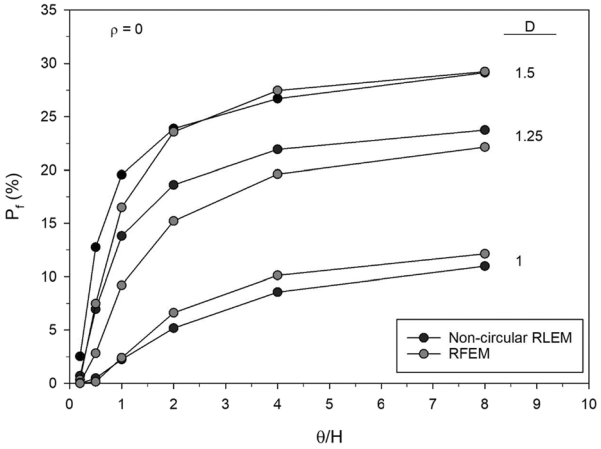

Fig. 13 Results of 2D non-circular RLEM and RFEM analyses of simple slopes with different D values and with linearly increasing undrained cohesion

As discussed in the introduction, a positive cross-correlation between cohesion and unit weight has been reported in the literature. Javankhoshdel et al. (2016) and Javankhoshdel and Bathurst (2016) reported a reduction in probability of failure when considering a reasonable maximum positive correlation value between undrained cohesion and unit weight (i.e. $\rho = 0.7$) for the case of simple slopes with spatial variability in soil parameters and using the circular RLEM or Single Random Variable Approach (SRV). This influence is re-examined in this study using a non-stationary random field for undrained cohesion and a stationary random field for unit weight. The results are presented in Fig. 14 using the non-circular RLEM. The same trends can be observed in this figure for both uncorrelated and cross-correlated random fields and different values of D. For example, probability of failure (P_f) increases with spatial correlation length as in the earlier figures. However, for the same spatial correlation length, the probability of failure decreases with decreasing depth ratio and the probability of failure is less for the case with $\rho = 0.7$.

7.3 Influence of Anisotropic 2D Spatial Variability on P_f ($r_{su} > 0$)

Anisotropic spatial variability for the case of linearly increasing undrained shear strength was also investigated together with correlated and uncorrelated strength and unit weight. Two cases of D = 1 and 1.25 were selected for this investigation. Figures 15 and 16 show the influence of anisotropic spatial correlation length on probability of failure using circular and non-circular RLEM analysis for different values of D, normalized vertical spatial correlation length θ_v/H, and constant $\theta_h/H = 1$. Data plots are presented in pairs with $\rho = 0$ and 0.7 in Figs. 15 and 16, respectively. Other parameters are given in the caption to the figure. It can be seen in these figures that for D = 1.25 (F_s = 1.55) there is a peak value of probability of failure, which occurs at normalized vertical spatial correlation length in the region of $0.5 \le \theta_v/H \le 0.75$ (the worst case spatial correlation length). This effect is more obvious in Fig. 16 for the case of $\rho = 0.7$. However, for D = 1 (F_s = 1.85), the probability of failure increases smoothly with increasing vertical spatial correlation length. The trends in the data for this case is

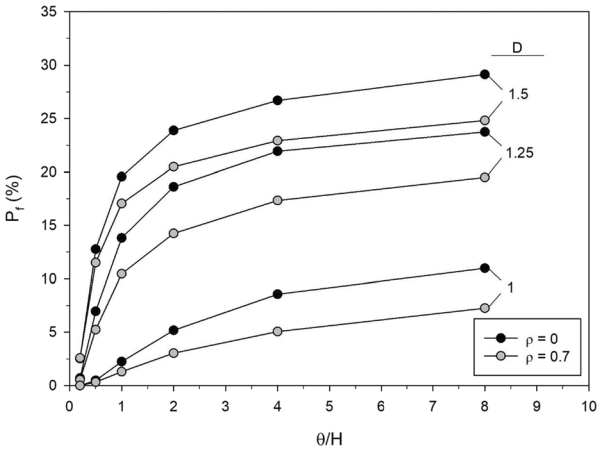

Fig. 14 Influence of positive correlation between undrained cohesion and unit weight on probability of failure using 2D non-circular RLEM approach

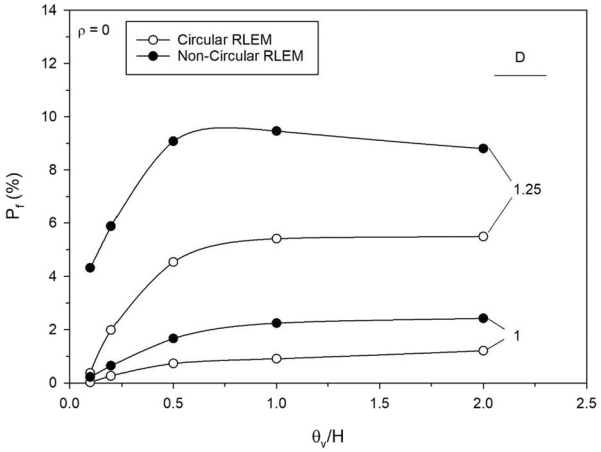

Fig. 15 Influence of anisotropic spatial correlation length on probability of failure using 2D circular and non-circular RLEM analysis for different values of D and F_s, $\theta_h/H = 1$, $COV_{su} = 0.5$, $COV_\gamma = 0.1$, $r_{su} = 1$and $\rho = 0$ and $M = 2$ and $\beta = 15°$

consistent with the practical maximum value of probability corresponding to stationary random soil strength conditions.

The trends in data in this figure are the same for both $\rho = 0$ and $\rho = 0.7$. However, as before, probabilities of failure are consistently lower for the case of positive cross-correlation. Fig. 17 shows the results with and without cross-correlation for the case on 2D non-circular RLEM analysis. It can also be seen in this figure that considering cross-correlation reduces the probability of failure. Also, as the spatial correlation length increases the difference between the values of probability of failure increases.

Figure 18 shows the corresponding mean F_s for different values of vertical spatial correlation length. It can be seen that having positive cross-correlation increases the mean F_s which is in contrary to the effect on the corresponding probability of failure as

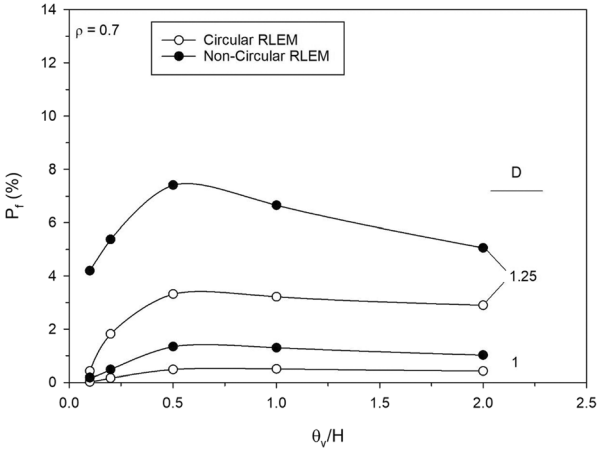

Fig. 16 Influence of anisotropic spatial correlation length on probability of failure using 2D circular and non-circular RLEM analysis for different values of D and F_s, $\theta_h/H = 1$, $COV_{su} = 0.5$, $COV_\gamma = 0.1$, $r_{su} = 1$and $\rho = 0.7$ and $M = 2$ and $\beta = 15°$

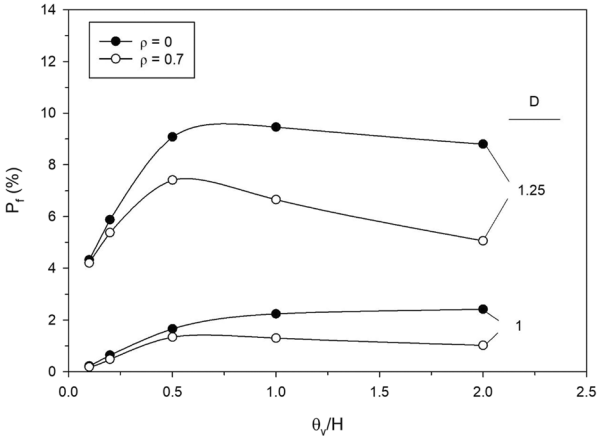

Fig. 17 Influence of anisotropic spatial correlation length on probability of failure using 2D non-circular RLEM analysis for different values of D and F_s, $\theta_h/H = 1$, $COV_{su} = 0.5$, $COV_\gamma = 0.1$, $r_{su} = 1$and $\rho = 0$ and $\rho = 0.7$ and $M = 2$ and $\beta = 15°$

illustrated in Fig. 17. Similar to Fig. 17, the same effect of increasing the difference between the values of mean F_s with increasing spatial correlation length can be seen in this figure. Figure 19 shows the results of probabilities of failure versus their corresponding mean factors of safety (results are taken from Figs. 16 and 17). Again, the deviation between the two cross-correlation scenarios increases by increasing the mean F_s. Also, the worst-case spatial correlation length is obvious for the case with $D = 1.25$.

Figure 20 is the comparison between the results of 2D non-circular RLEM and 2D RFEM for the case of anisotropic spatial correlation length for $\rho = 0$. It can be noticed that the probability of failure increases with the heterogeneity anisotropy. Jamshidi Chenari and Alaie (2015) reported a dual effect on probability of failure of natural earth slopes. Depending on the deterministic safety factor, the reliability index would either increase or decrease with the anisotropy of spatial correlation length. However,

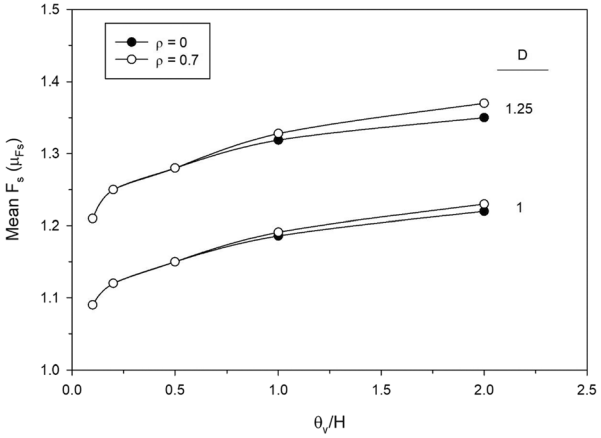

Fig. 18 Influence of anisotropic spatial correlation length on mean factor of safety using 2D non-circular RLEM analysis for different values of D and F_s, $\theta_h/H = 1$, $COV_{su} = 0.5$, $COV_\gamma = 0.1$, $r_{su} = 1$ and $\rho = 0$ and $\rho = 0.7$ and $M = 2$ and $\beta = 15°$

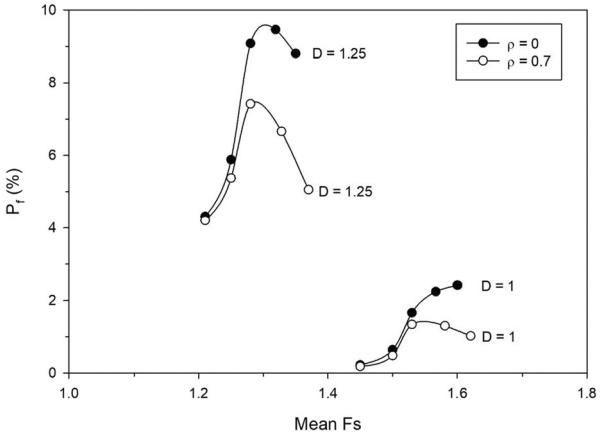

Fig. 19 P_f vs mean F_s for the results of non-circular RLEM analysis for different values of D and F_s, $\theta_h/H = 1$, $COV_{su} = 0.5$, $COV_\gamma = 0.1$, $r_{su} = 1$and $\rho = 0$ and $\rho = 0.7$ and $M = 2$ and $\beta = 15°$

Jamshidi Chenari and Alaie (2015) adopted an inversed definition for the anisotropy ratio by assuming a constant vertical correlation length. For the cases presented in Fig. 18, the deterministic safety factor corresponds to the values of 1.47 and 1.76 for D = 1 and 1.25, respectively. So, results consistent with the literature are found in this study.

It is further observed from this figure that the difference between the results of 2D non-circular RLEM and 2D RFEM is negligible, i.e. the 2D non-circular RLEM can find the same weakest failure path as 2D RFEM.

7.4 Layered Slopes ($r_{su} > 0$)

Four different cases are investigated for a two-layer slope with linearly increasing undrained cohesion in both layers (i.e. bi-linear strength) and isotropic spatial

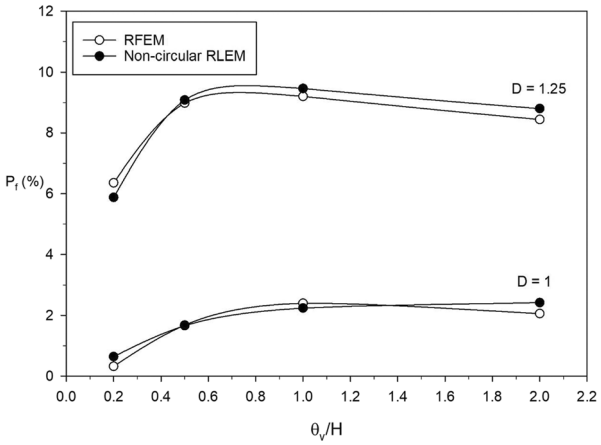

Fig. 20 Influence of anisotropic spatial correlation length on probability of failure using 2D non-circular RLEM and 2D RFEM analysis for different values of D and F_s, $\theta_h/H = 1$, $COV_{su} = 0.5$, $COV_\gamma = 0.1$, $r_{su} = 1$ and $\rho = 0$ and $M = 2$ and $\beta = 15°$

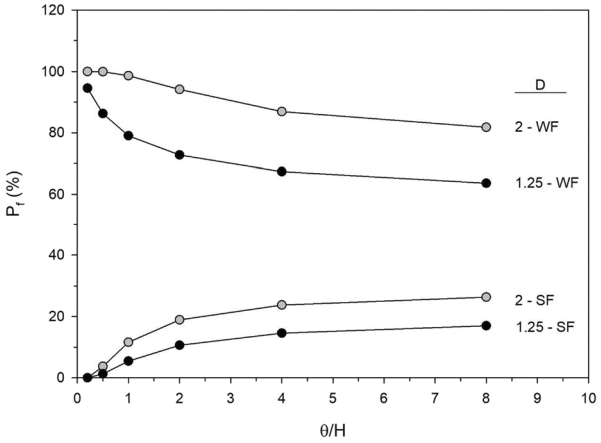

Fig. 21 Influence of spatial variability of soil properties on probability of failure for four different two-layer slope cases (D = 1.25 with weak and strong foundation, and D = 2 with weak and strong foundation) using 2D non-circular RLEM approach

variability. The four cases are (1) D = 1.25 with weak foundation; (2) D = 1.25 with strong foundation; (3) D = 2 with weak foundation; and (4) D = 2 with strong foundation as shown in Fig. 2.

Figure 21 shows values of probability of failure for different spatial correlation length for all cases. It can be seen in this figure that the trend in data for cases 1 and 3 (top curves with weak foundation) is different from cases 2 and 4 with strong foundation. Specifically, for the cases of 1 and 3, as spatial correlation length decreases P_f increases and the largest correlation length in this figure (θ/H = 8, which approximates the case of infinite spatial variability) gives a minimum probability of failure. However, for the cases of 2 and 4, the trend is the opposite, and θ/H = 8 corresponds to the maximum probability of failure when all other conditions remain the same. Also, as

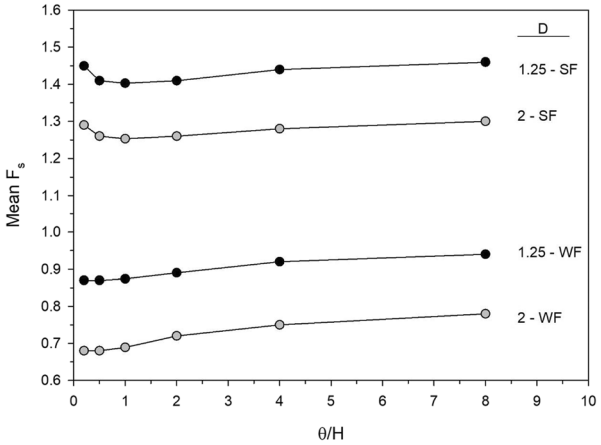

Fig. 22 Influence of spatial variability of soil properties on mean F_s for four different two-layer slope cases (D = 1.25 with weak and strong foundation, and D = 2 with weak and strong foundation) using 2D non-circular RLEM approach. (WF = soil unit weight gradient and SF = soil cohesion gradient in the foundation)

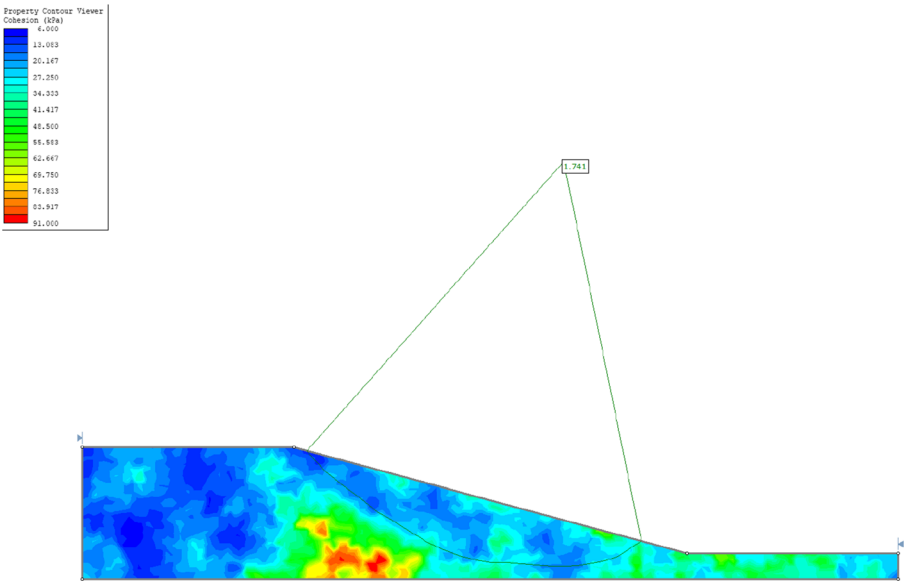

Fig. 23 An example of a non-circular RLEM failure surface D = 1.25 and $F_s = 1.74$, $\theta_h/H = 1$, $\theta_v/H = 1$, $COV_{su} = 0.5$, $COV_\gamma = 0.1$, $r_{su} = 1$ and $\rho = 0$ and M = 2 and $\beta = 15°$

it was mentioned earlier that the case with D = 2 gives higher probability of failure compared with the case with D = 1.25 and the same spatial correlation length.

Figure 22 shows the values of mean F_s corresponding to the P_f values illustrated in Fig. 21 against the spatial correlation length for all cases. In this figure, case 2 (D = 1.25 with strong foundation) has the highest mean F_s, and case 3 (D = 2 with weak foundation) has the lowest value of mean F_s for the same spatial correlation length. Cases 1 and 3 also have mean F_s less than 1 for small values of spatial correlation length. For each case, there is an overall trend of decreasing mean F_s value with decreasing spatial correlation. However, this rate of change is small and the mean F_s value for each plot in this figure varies over a small range and thus is not of practical concern.

This study was the first attempt to model a two-layer slope with non-circular analysis and using SAO technique. This method can easily model more complicated geometries and to help researchers to grasp the concept of spatial variability and seeking out the weakest path better. Figure 23 shows an example of finding the failure mechanism using the 2D non-circular RLEM for the isotropic spatial variability. This figure clearly shows the non-circular failure mechanism avoiding the strong region and trying to find the weakest path which is impossible to seek using circular analysis.

8 Conclusions

Probabilistic analysis of slopes with constant mean (stationary) and linearly increasing mean (non-stationary) undrained shear strength was investigated using the 2D random limit equilibrium method (RLEM) and considering both isotropic and anisotropic

spatial variability of soil properties and cross-correlation between soil strength (s_u) and unit weight (γ). The Morgenstern-Price method was used in the 2D RLEM analyses. Random field theory (LAS method) was used to generate both correlated and uncorrelated random fields with spatial variability of soil properties. The following are the main conclusions of the current study.

1. The paper shows that for the case of homogenous soil properties (i.e. random variability only), the FOSM solution by Javankhoshdel and Bathurst (2016) can be used together with the design charts from Griffiths and Yu (2015) to calculate the probability of failure of simple slopes with constant and linearly increasing mean undrained shear strength together with cross-correlation of soil properties. For these cases, increasing the positive correlation between s_u and γ reduces the probability of failure.
2. For constant COV of soil undrained shear strength and unit weight, and cross-correlation coefficient (ρ), the probability of failure varies essentially linearly with the log value of deterministic safety factor F_s computed using the Griffiths and Yu (2015) charts.
3. Numerical outcomes for slopes with isotropic spatial variability showed that increasing positive cross-correlation between s_u and γ random fields decreases the probability of failure for the same slope geometry and normalized spatial correlation length.
4. Non-circular RLEM which is a combination of Morgenstern-Price algorithm, SAO technique and LAS method to model spatial variability gives higher probability of failure compared with the circular RLEM. The non-circular RLEM has the ability to seek out the weakest failure path in slopes with spatial variable soil properties.
5. For the simple slopes in this study with non-stationary, and the isotropic and anisotropic spatial variabilities of undrained shear strength, there was an evident peak in probability of failure for the steepest slope cases at low normalized spatial correlation lengths. The maximum peak probability was seen to occur at greater normalized spatial correlation length as slope angles decreased and for practical purposes approached the probability of failure computed for slopes with infinite spatial variability (i.e. random variability only).
6. Probability of failure for the simple slopes with non-stationary and anisotropic soil spatial variability in this study was more sensitive to changes in vertical spatial correlation length than horizontal spatial correlation length.

The practical value of this study is to demonstrate that deterministic design charts for simple slopes with constant and linearly increasing undrained shear strength and margins of safety expressed in terms of conventional factors of safety can be used to compute margins of safety in probabilistic terms. The latter can serve as a complementary tool for designers who are most accustomed to the assessments of slope stability based on the conventional factors of safety.

A common concern with geotechnical engineers is the mismatch between computed probabilities of failure for simple slopes in comparison with the expectations inspired by experience based on the conventional factors of safety computed from deterministic limit equilibrium methods. The results of analyses in this paper show that margins of safety in both deterministic and probabilistic terms can be brought into closer alignment

by considering both positive cross-correlations between soil properties and small spatial correlation lengths.

Finally, a few cases are presented in this study to demonstrate that probabilities of failure computed using 2D non-circular RLEM and 2D RFEM can be in satisfactory agreement in some cases and there are cases that 2D non-circular RLEM gives higher probability of failure compared to 2D RFEM. Currently, the use of 2D RFEM for slope stability analyses is restricted to the research literature. The interested reader is directed to the paper by Javankhoshdel et al. (2016) for more comprehensive investigations of the differences in numerical outcomes using both approaches.

Acknowledgements The authors would like to thank Rocscience Inc. for the time and computational tools that have been provided by the company to the authors.

Author Contributions The first and fourth authors have contributed to this paper by doing the RLEM analyses. To be more specific, mainly Dr. Javankhoshdel and occasionally Mr. Dastpak have carried out the whole Slide2 analyses in order to generate raw materials for this research publication. Furthermore, Dr. Javankhoshdel and Miss Cami have jointly drawn the illustrations and written the manuscript. Last, but not least, Prof. Jamshidi Chenari has checked the results, contributed to the interpretations and read and edited the manuscript both technically and editorially. He is also the corresponding author.

Availability of Data and Material (Data Transparency) Not applicable.

Compliance with Ethical Standards

Declarations To be used for non-life science journals: Not applicable.

Conflicts of Interest There are no conflicting/competing interests in this paper.

Code Availability (Software Application or Custom Code) Not applicable.

References

Bjerrum, L.: Geotechnical properties of Norwegian marine clays. Geotechnique. **4**(2), 49–69 (1954)

Ching, J., Phoon, K.K., Hu, Y.G.: Efficient evaluation of reliability for slopes with circular slip surfaces using importance sampling. ASCE J. Geotech. Geoenviron. Eng. **135**(6), 768–777 (2009)

Cho, S.E.: Probabilistic assessment of slope stability that considers the spatial variability of soil properties. ASCE J. Geotech. Geoenviron. Eng. **136**(7), 975–984 (2010)

Chowdhury, R.N., Xu, D.W.: Rational polynomial technique in slope reliability analysis. ASCE J. Geotech. Geoenviron. Eng. **119**(12), 1910–1928 (1993)

Christian, J.T., Ladd, C.C., Baecher, G.B.: Reliability applied to slope stability analysis. ASCE J. Geotech. Geoenviron. Eng. **120**(12), 2180–2207 (1994)

El-Ramly, H., Morgenstern, N.R., Cruden, D.M.: Probabilistic slope stability analysis for practice. Can. Geotech. J. **39**, 665–683 (2002)

Fenton, G.A., Vanmarcke, E.H.: Simulation of random fields via local average subdivision. J. Eng. Mech. **116**(8), 1733–1749 (1990)

Gibson, R.E., Morgenstern, N.: A note on the stability of cuttings in normally consolidated clay. Géotechnique. **12**(3), 212–216 (1962)

Greco, V.R. 1996. Efficient Monte Carlo technique for locating critical slip surface. Journal of Geotechnical Engineering, Vol. 122, No. 7, July 1996

Griffiths, D.V., Fenton, G.A.: Probabilistic slope stability analysis by finite elements. ASCE J. Geotech. Geoenviron. Eng. **130**(5), 507–518 (2004)

Griffiths, D.V., Huang, J.S., Fenton, G.A.: Influence of spatial variability on slope reliability using 2-D random fields. ASCE J. Geotech. Geoenviron. Eng. **135**(10), 1367–1378 (2009)

Griffiths, D.V., Huang, J.S. and Fenton, G.A. 2015. Probabilistic slope stability analysis using RFEM with non-stationary random fields. Proceedings of the Fifth International Symposium on Geotechnical Safety and Risk (ISGSR2015), Rotterdam, the Netherlands. Page: 690–695

Griffiths, D.V., Yu, X.: Another look at the stability of slopes with linearly increasing undrained strength. Géotechnique. **65**(10), 824–830 (2015)

Hassan, A.M., Wolff, T.F.: Search algorithm for minimum reliability index of earth slopes. ASCE J. Geotech. Geoenviron. Eng. **125**(4), 301–308 (1999)

Hong, H., Roh, G.: Reliability evaluation of earth slopes. ASCE J. Geotech. Geoenviron. Eng. **134**(12), 1700–1705 (2008)

Hunter, J.H., Schuster, R.L.: Stability of simple cuttings in normally consolidated clay. Géotechnique. **18**(3), 372–378 (1968)

Jamshidi Chenari, R., Zhalehjoo, N., Karimian, A.: Estimation on bearing capacity of shallow foundations in heterogeneous deposits using analytical and numerical methods. Scientia Iranica. **21**(3), 515–505 (2014)

Jamshidi Chenari, R., Mahigir, A.: The effect of spatial variability and anisotropy of soils on bearing capacity of shallow foundations. Civil. Eng. Infrastruct. J. **47**(2), 199–213 (2014)

Jamshidi Chenari, R., Alaie, R.: Effects of anisotropy in correlation structure on the stability of an undrained clay slope. J. Geotech. Geoenviron. Eng. **9**(2), 109–123 (2015)

Jamshidi Chenari, R. and Zamanzadeh, M., 2016. Uncertainty assessment of critical excavation depth of vertical unsupported cuts in undrained clay using random field theorem. Scientia Iranica. Transaction A, Civil Engineering, 23(3), p.864

Javankhoshdel, S., Bathurst, R.J.: Simplified probabilistic slope stability design charts for cohesive and c-ϕ soils. Can. Geotech. J. **51**(9), 1033–1045 (2014)

Javankhoshdel, S., Bathurst, R.J.: Influence of cross-correlation between soil parameters on probability of failure of simple cohesive and c-ϕ slopes. Can. Geotech J. (online). **53**, 839–853 (2016). https://doi.org/10.1139/cgj-2015-0109

Javankhoshdel, S.: Reliability analysis of simple slopes and soil-structures with linear limit states, PhD Dissertation. Queen's University, Kingston, Canada (2016)

Javankhoshdel, S., Luo, N. and Bathurst, R.J. 2016. Probabilistic analysis of simple slopes with cohesive soil strength using RLEM and RFEM. J. Geotech. Geoenviron. Eng. (online). https://doi.org/10.1080/17499518.2016.1235712

Koppula, S.D.: On stability of slopes in clay with linearly increasing strength. Can. Geotech. J. **21**(3), 577–581 (1984)

Li, D.Q., Qi, X.H., Phoon, K.K., Zhang, L.M., Zhou, C.B.: Effect of spatially variable shear strength parameters with linearly increasing mean trend on reliability of infinite slopes. Struct. Saf. **49**, 45–55 (2014)

Li, K.S., Lumb, P.: Probabilistic design of slopes. Can. Geotech. J. **24**, 520–535 (1987)

Low, B., Gilbert, R., Wright, S.: Slope reliability analysis using generalized method of slices. ASCE J. Geotech. Geoenviron. Eng. **124**(4), 350–362 (1998)

Low, B.K. 2003. Practical probabilistic slope stability analysis. Proceedings, Soil and Rock America 2003, 12th Panamerican Conference on Soil Mechanics and Geotechnical Engineering and 39th U.S. Rock Mechanics Symposium, M.I.T., Cambridge, Massachusetts, June 22–26, 2003, Verlag Glückauf GmbH Essen, 2: 2777–2784

Low, B.K., Lacasse, S., Nadim, F.: Slope reliability analysis accounting for spatial variation. J. Geotech. Geoenviron. Eng. **1**(4), 177–189 (2007)

Mbarka, S., Baroth, J., Ltifi, M., Hassis, H., Darve, F.: Reliability analyses of slope stability: homogeneous slope with circular failure. Eur. J. Environ. Civ. Eng. **14**(10), 1227–1257 (2010)

Mostyn, G. R. and Soo, S. 1992. The effect of autocorrelation on the probability of failure of slopes. In 6th Australia, New Zealand Conference on Geomechanics: Geotechnical Risk: 542–546

Nguyen, V.U., Chowdhury, R.N.: Simulation for risk analysis with correlated variables. Geotechnique. **35**(1), 47–58 (1985)

Phoon, K.K., Kulhawy, F.H.: Characterization of geotechnical variability. Can. Geotech. J. **36**(4), 612–624 (1999)

Ranjbar Pouya, K., Zhalehjoo, N., Jamshidi Chenari, R.: Influence of random heterogeneity of cross-correlated strength parameters on bearing capacity of shallow foundations. Indian Geotech. J. **44**(4), 427–435 (2014)

Rocscience, 2018. Slide2 2018: 2D Limit Equilibrium Slope Stability Analysis. https://www.rocscience.com/software/slide2

Shah Malekpoor, P., Jamshidi Chenari, R., Javankhoshdel, S.: Discussion of "probabilistic seismic slope stability analysis and design". Can. Geotech. J. **999**, 1–6 (2020)
Shen, J.M., Brand, E.W.: Discussion of 'on stability of slopes in clay with linearly increasing strength' by Koppula, S.D. Can. Geotech. J. **22**(3), 419–421 (1985)
Sivakumar Babu, G.L., Mukesh, M.D.: Effect of soil variability on reliability of soil slopes. Geotechnique. **54**(5), 335–337 (2004)
Sivakumar Babu, G.L., Srivastava, A.: Reliability analysis of allowable pressure on shallow foundation using response surface method. Comput. Geotech. **34**(3), 187–194 (2007)
Tabarroki, M., Ahmad, F., Banaki, R., Jha, S., Ching, J.: Determining the factors of safety of spatially variable slopes modeled by random fields. ASCE J. Geotech. Geoenviron. Eng. **139**(12), 2082–2095 (2013)
Taylor, D.W.: Stability of earth slopes. J. Boston Soc. Civ. Eng. **24**(3), 197–246 (1937)
Wang, Y., Cao, Z.J., Au, S.K.: Practical reliability analysis of slope stability by advanced LHS simulations in a spreadsheet. Can. Geotech. J. **48**(1), 162–172 (2011)
Yu, H.S., Salgado, R., Sloan, S.W., Kim, J.M.: Limit analysis versus limit equilibrium for slope stability. J. Geotech. Geoenviron. Eng. **124**(1), 1–11 (1998)
Zhu, D., Griffiths, D.V., Huang, J., Fenton, G.A.: Probabilistic stability analyses of undrained slopes with linearly increasing mean strength. Géotechnique. **67**(8), 733–746 (2017)

Affiliations

Sina Javankhoshdel[1] · Brigid Cami[2] · Reza Jamshidi Chenari[3] · Pooya Dastpak[4]

Sina Javankhoshdel
sina.javankhoshdel@rocscience.com

Brigid Cami
Brigid.Cami@rocscience.com

Pooya Dastpak
p.dastpak@mail.um.ac.ir

[1] Geomechanics Specialist, Rocscience Inc., 54 St. Patrick st., Toronto, Ontario, Canada

[2] Geotechnical Software Developer, Rocscience Inc., 54 St. Patrick st, Toronto, Ontario, Canada

[3] Associate Professor, Department of Civil Engineering, Faculty of Engineering, University of Guilan, Rasht, Guilan, Iran

[4] M.Sc. Graduate, Department of Civil Engineering, Faculty of Engineering, Ferdowsi University of Mashhad, Mashhad, Iran